Wear resistance of WCp/Duplex Stainless Steel metal matrix composite layers prepared by laser melt injection

Do Nascimento, A. M.; Ocelik, V.; Ierardi, M. C. F.; De Hosson, J. Th. M.

Published in:
Surface & Coatings Technology

DOI:
10.1016/j.surfcoat.2008.04.061

Available online at www.sciencedirect.com
ScienceDirect
Surface & Coatings Technology 202 (2008) 4758–4765
SURFACE & COATINGS TECHNOLOGY
www.elsevier.com/locate/surfcoat

Wear resistance of WC_p/Duplex Stainless Steel metal matrix composite layers prepared by laser melt injection

A.M. Do Nascimento [a], V. Ocelík [b,*], M.C.F. Ierardi [a], J.Th.M. De Hosson [b]

[a] Department of Materials Science, Faculty of Mechanical Engineering, State University of Campinas, UNICAMP, P.O. Box 6122, 13083-970 Campinas-SP, Brazil
[b] Department of Applied Physics, Materials Innovation Institute, University of Groningen, Nijenborgh 4, 9747 AG Groningen, The Netherlands

Received 30 January 2008; accepted in revised form 7 April 2008
Available online 18 April 2008

Abstract

Laser Melt Injection (LMI) was used to prepare metal matrix composite layers with a thickness of about 0.7 mm and approximately 10% volume fraction of WC particles in three kinds of Cast Duplex Stainless Steels (CDSSs). WC particles were injected into the molten surface layer using Nd:YAG high power laser beam. As a result the microstructure characterized by hard ceramic particles distributed in a metal matrix with the strong bonding to substrate is formed in the surface layer of the treated metal.

Dry sliding wear properties of these metal matrix composites layers were measured and compared with the wear properties of the substrate and with surfaces simply remelted by the laser beam. The observed wear mechanisms are summarized and related to detailed microstructural observations. The layers have been found to show excellent interfacial bonding, coupled with substantially improved tribological properties expressed through the wear resistance increase of 8 times. The amount of WC particles was sufficient to reinforce the matrix and the particles have shown a good bonding to the matrix to support the contact stress in the layer.

Keywords: Laser treatment; Metal Matrix Composites; Wear; Duplex Stainless Steel

1. Introduction

It is well known that Cast Duplex Stainless Steels (CDSSs) have excellent corrosion resistance and good mechanical strength. However, poor hardness and wear resistance [1] limit the range of application. Various attempts were made to process these alloys over a wide range of surface engineering methodologies to remove this drawback. One of these surface engineering techniques is the Laser Melt Injection (LMI) technique, in which the high power laser locally melts a top part of metal substrate whilst, simultaneously, strengthening particles are injected into the melt pool and trapped by rapid solidification [2].

This method is accordingly suited to form up to 1 mm thick Metal Matrix Composite (MMC) layers on the top of a metal work-piece improving the mechanical and tribological properties of the surface [3]. The properties of the produced MMC layer depend on, among other things, the amount of the injected powder, the microstructure of the melt pool matrix and the bonding between particle and matrix. Many kinds of ceramic particles reinforced surfaces of metallic materials have been produced by LMI. Some examples are SiC/Al [4], SiC/Al8Si [3], WC/Ti6Al4V [5], SiC/Ti6Al4V [6] and SiC/Mg-alloy [7]. Recently the injection of WC particles into the surface of a low carbon steel with an assistance of a plasma arc as heat source was also reported [8]. MMC layers formed by injection of fine powders contain a sufficient amount of ceramic particles to reinforce the matrix and to improve substantially the sliding wear resistance in comparison with the substrates. Despite a promising performance of the created MMC coatings, the processing windows in which these coatings can be administered are small due to an intensive heating and melting of the particles within the laser beam and consecutive formation of harmful phases, which may lead to matrix embrittlement and cracking.

In the previous paper [9] microstructural features after LMI of multigrain WC particles into the surface of three selected

* Corresponding author. Tel.: +31 503633407; fax: +31 503634881.
E-mail address: V.Ocelik@rug.nl (V. Ocelík).

0257-8972/$ - see front matter © 2008 Elsevier B.V. All rights reserved.
doi:10.1016/j.surfcoat.2008.04.061

duplex steels have been studied. Although after simple laser surface remelting the austenitic phase is almost absent inside remelted layer, in the case of LMI austenitic phase was observed in the vicinity of WC particles, due to increase of carbon content coming from dissolved particles and acting as austenite stabilizer. The diffusion of carbon in the reaction zone between WC particle and liquid melt results in a formation of W_2C phase in the neighborhood of WC particles showing a strong orientation relationship with them. The maximum volume fraction of the particles achieved in the metal matrix composite layer was about 10% and a substantial increase in hardness was observed, i.e. 575 HV0.2 for the matrix with embedded particles in comparison to 290 HV0.2 for untreated cast duplex stainless steels.

The aim of the present paper is to address the wear and friction characteristics of the MMC layers created by laser melt injection of WC particles into surface of these three duplex steels. Although enhancement of surface properties of different metals and alloys by laser melt injection is not a new technique, the novelty of this study lies in the fact that for the first time the laser melt injection technique has been used in improving the surface properties of duplex steels. Together with the previous paper [9] it will form an integrated view onto the microstructure, wear resistance and corrosion resistance changes of duplex steel surfaces treated by LMI of WC particulates.

2. Experimental details

Three types of CDSSs (see Table 1) were used as substrates for preparation of overlapping tracks of WC_p/CDSSs MMC layers by the LMI technique using a 2 kW Rofin Sinar Nd:YAG laser. Globular multigrain WC particles with a mean size of 80 μm were injected under LMI processing conditions. The width of the coated circular area was more than 4 mm, formed by 15–20% overlapping of the spiral type of laser track. Two circular coated areas were created on one disk 50 mm in diameter; inner one with average radial distance of 9.6 mm and external one with average radial distance of 16.7 mm. Fig. 1 shows an example of duplex steel disk after formation of these two circular coatings by LMI. A more detailed description of the LMI process, with particular reference to the process parameters as well as detailed description of microstructures and particle distributions formed inside WC_p/CDSSs layers can be found in [9].

Standard light microscopy (Olympus Vanox-AHTM), Scanning Electron Microscopy with integrated EDS (SEM Philips XL30 FEG) and confocal microscopy were used to study particle distribution and wear micromechanisms, to analyze the metal debris and oxides and to observe worn surfaces of WC_p/CDSS layers.

Table 1
The chemical composition (in wt.%) of the three types of CDSSs: ASTM A890 grade 1A (free of nitrogen), ASTM A890 grade 3A (with nitrogen and without Cu) and ASTM A890 grade 6A (Super Duplex)

Alloy	C	Cr	Ni	Mn	Si	Mo	S	P	Cu	N	W
1A	0.04	25.01	5.53	0.78	0.99	2.11	0.006	0.026	3.10		
3A	0.03	25.33	5.38	0.84	0.90	2.13	0.005	0.025		0.19	
6A	0.02	25.96	7.93	0.83	0.97	3.63	0.008	0.024	0.82	0.24	0.78

All compositions are balanced to 100% by iron.

Fig. 1. Two circular coated areas on 50 mm diameter duplex steel disk formed by an overlapping of the spiral type of LMI laser tracks.

The wear resistance of MMC layers during dry sliding wear was investigated using a CSM HT tribometer in pin-on-disc wear test. A High-speed steel M-42 pin with hardness of about 950 HV and dimensions of 2×3 mm^2 is loaded with the force of 15 N against rotating discs with CDSS substrates and two MMC circular area coatings on them. The disc rotates with a tangential speed of 10 cm/s, while the pin was placed at a distance of 9.6 or 16.7 mm from the center of the disc. The wear test was stopped after 10,000 laps. In this configuration an area of pin is continuously in contact with coating, whereas the corresponding areas of the coating are only in contact once during a lap. The wear rate is in this case defined as a wear volume per unit track length, per unit of normal load and per lap [10]. Even though the calculated value of the wear rate according to this definition is exactly the same as that calculated from the total sliding distance of the pin (equal to the product of laps and perimeter of the wear track), its physical meaning is different from the commonly used dimension "m^3/(N m)" of wear rate that only counts for the configuration of pin sample sliding against a disc as the reference material. The level of relative humidity was measured but not controlled and it was always between 30 and 40%. All wear tests were carried out at room temperature.

3. Results

Three types of samples were tested under dry sliding conditions; CDSS surfaces without any laser treatment, CDSS surfaces treated by laser remelting (using the same processing parameters as during LMI) and CDSS surfaces with injected WC particles. The main microstructural differences in these samples were observed and concluded in previous paper [9]. The coarse ferritic grains with a size ranging from 0.5 to 1 mm containing a couple of hundreds of austenitic dendrites with a mean size of 30 μm is the characteristic microstructure of all non-treated surfaces (see Fig. 1 in [9]). The content of austenitic phase measured by orientation image microscopy (OIM) is almost the same (about 50%) for 1A and 3A alloy, and slightly

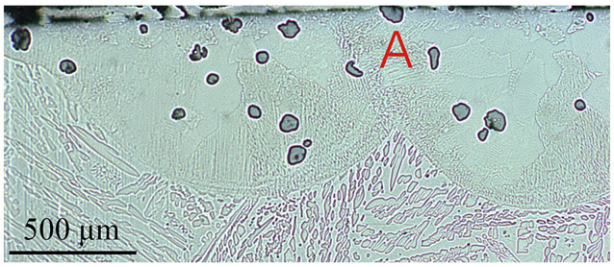

Fig. 2. Optical micrograph from transversal cross-section of two adjacent laser tracks of WC_p/CDSS prepared by laser melt injection into 6A showing the overlapping area highlighted by letter A.

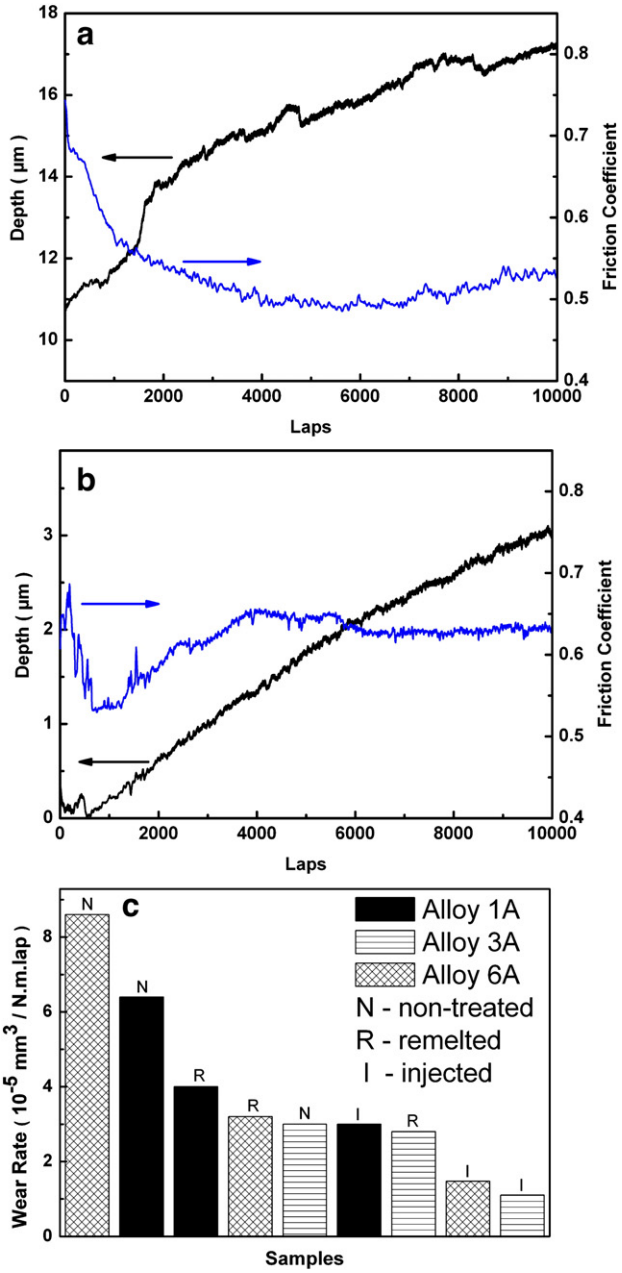

Fig. 3. Depth position of pin and friction coefficient versus number of laps on (a) a non-treated 3A CDSS surface and (b) the same surface after LMI; c) Wear rates for non-treated (N), remelted (R) and particle injected (I) surfaces of all three CDSS alloys calculated from the slope of wear curve.

lower (43%) for 6A alloy. After laser surface remelting the predominance of the ferritic phase was confirmed by OIM and X-ray diffraction for all three duplex steels. Finally, Fig. 2 illustrates the microstructure of 6A sample on the transversal cross-section after LMI.

WC particles are randomly distributed in the surface layer with a volume density 8–10%. Partial dissolution of WC particles forms in their immediate neighborhood new microstructural features containing small W_2C islands, Fe–$(Fe,W)_xC$ eutectics with different amount of W [11] and austenitic dendrites [9].

Fig. 3a shows a typical performance during the wear test performed on non-treated 3A alloy surface at temperature 25 °C. The depth position of the pin and the friction force are continuously registered during 10,000 disc rotations.

In all measurements on non-treated surfaces the initial "running-in" period is observed (about 2000 cycles), after which a constant wear rate process is established. The wear rate in the transition region is relatively high and accompanied with a higher friction coefficient (>0.6). During the running-in period, the friction force decreases and in the period of stable wear rate it is more or less constant. Fig. 3b shows the result of the wear test of 3A sample with injected particles. The running-in period is longer, but a stable wear rate period is also established. The wear rate can be easily estimated from the

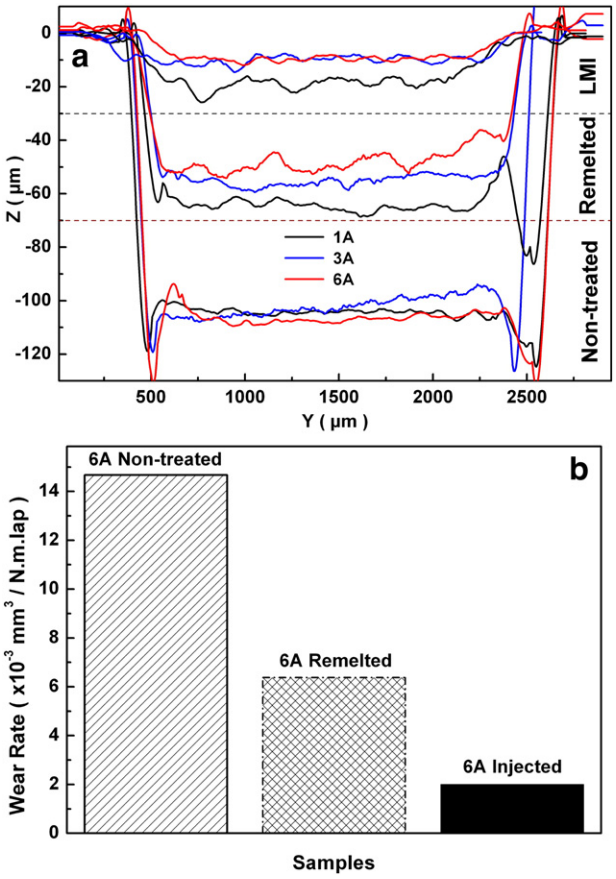

Fig. 4. a) Depth profiles of worn surfaces after dry sliding wear tests performed on treated and non-treated surfaces. b) Wear rate calculated from worn depth measurements for 6A alloy samples.

slope of the part of the depth curve after the transition period. These calculations are summarized in Fig. 3c where a comparison of wear rates of non-treated and treated surfaces is depicted of all three alloys.

Fig. 3c clearly demonstrates that laser surface remelting and LMI of WC particles into CDSS surface improve always the wear resistance. However, after remelting of 3A alloy the improvement in wear resistance is not so significant as for the remelted and injected surfaces of 1A alloy. Generally, it is observed that the surface after LMI is more resistant against sliding wear than a remelted surface. The remelted one is more resistant than the non-treated one for each tested alloy.

However, it is well known that the estimation of wear rate just from the pin position during sliding wear test can be connected with a large error due to the wear of pin itself, especially for more wear resistant surfaces. This was the main reason, why a decision has been made to compare the wear resistance of treated and non-treated surfaces by another method. Fig. 4a shows the shapes of worn profiles measured by confocal microscope transversally to the pin sliding direction after 10,000 laps on all three duplex steel surfaces.

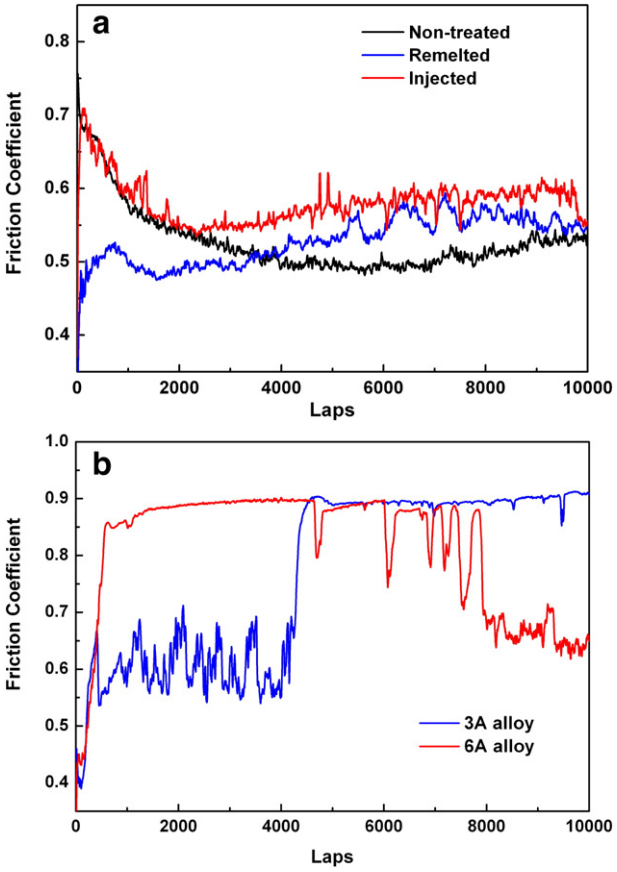

Fig. 5. Friction coefficient versus number of laps during sliding with velocity of 10 cm/s and 15 N applied load. a) All three conditions of 1A alloy sliding against an HSS pin showing the same behavior of the coefficient friction. b) Non-stable behavior of coefficient of friction during sliding wear tests of injected surfaces on inner circular area.

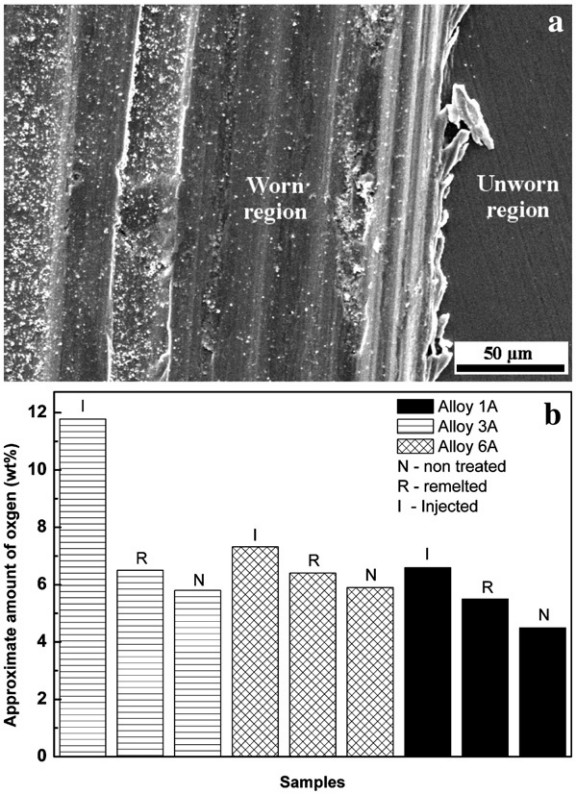

Fig. 6. a) SEM of 1A alloy surface after wear test showing the worn region, the wear direction, the plastic deformation in the wear track edge and the unworn region. b) Approximate amount of the oxygen detected by EDS on the worn surfaces after dry sliding wear test.

These depth profiles clearly classify the wear resistance of all surfaces into three groups. Non-treated surfaces have shown the lowest wear resistance due to the highest depth of worn groove on a level of about 105 µm. There is no significant difference between average depths of worn groove for all three duplex steel surfaces. On the remelted surfaces the final depth of worn groove is reduced to values between 40 and 65 µm and on the injected surfaces further to values between 8 and 20 µm. For remelted and injected surfaces a difference between individual

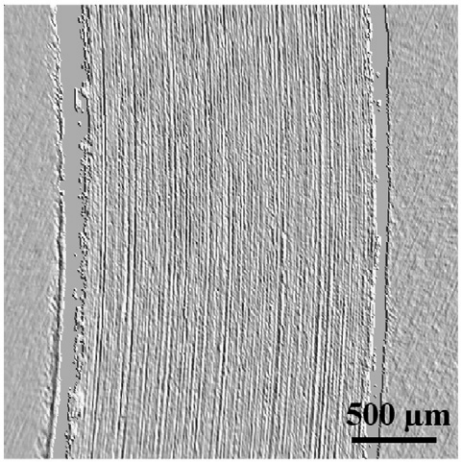

Fig. 7. Photo-realistic image created by confocal microscopy of the worn surface of 1A alloy tested in the non-treated condition.

alloys is detected in a sense that alloy 1A shows after remelting and injection the lowest wear resistance.

To quantify the wear resistance from this observation, the depth profiles were measured after 10,000 laps on several places of each worn groove, averaged and subsequently the worn volume was estimated. Results of these calculations for 6A alloy are summarized in Fig. 4b. Now a substantial difference in the wear rate between a non-treated and injected surface is clearly visible. Wear rate on 6A alloy surface is reduced more then seven times after laser melt injection.

Fig. 5 shows the behavior of the friction coefficient during the wear test. Fig. 5a displays this behavior for all three surface conditions: injection, remelting and non-treated surface of 1A alloy. All three surfaces have shown a friction coefficient between 0.5 and 0.6 after some transition period (~2000 laps). The non-treated and injected surface exhibit at the beginning a higher value of CoF while on the remelted surface the onset value of the CoF is much lower.

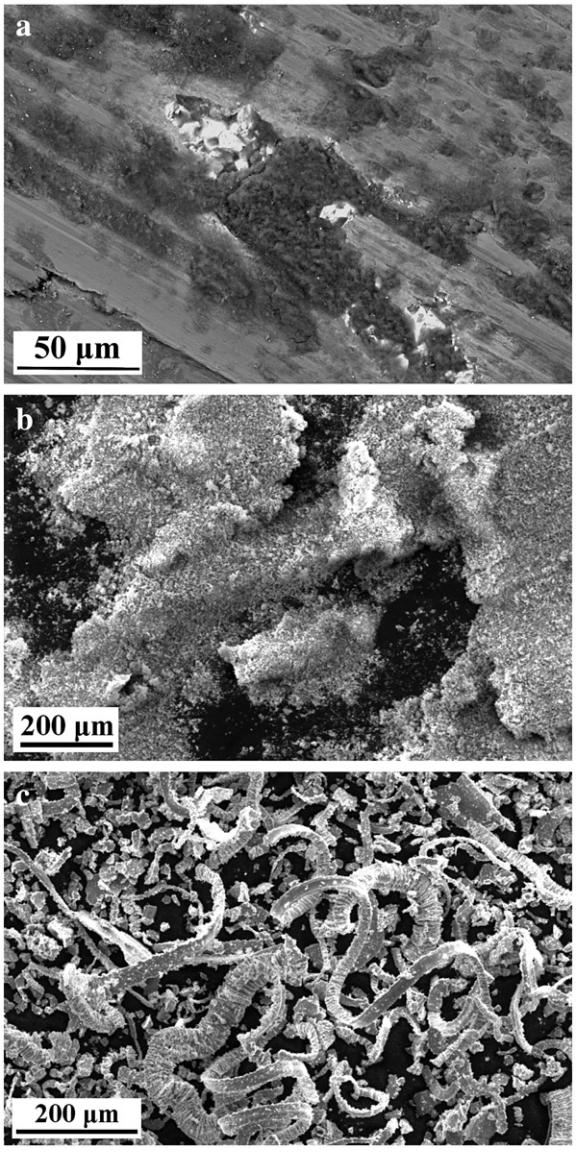

Fig. 8. SEM micrographs showing: a) BSE image of oxides (darker regions) close to WC particles (brighter regions); b) SE image of debris formed on injected surface; c) SE image of debris formed on non-treated surface.

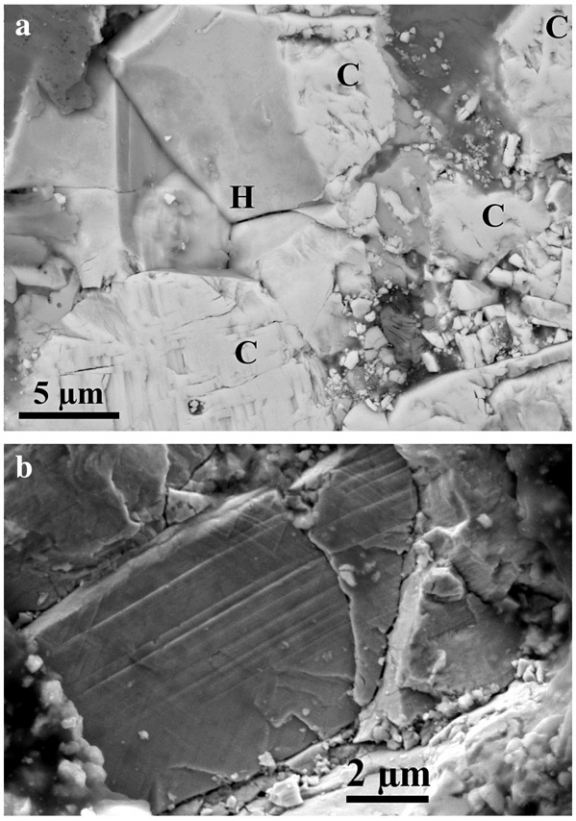

Fig. 9. a) SEM micrograph exhibiting the intergranular fracture on WC multi-grain particle in the vicinity of grains in sliding contact. H marks the hole after intergranular fracture, C shows the surfaces in sliding contact. b) SEM micrograph showing the signs of plastic deformation accumulated in WC grain.

However, some tests performed on the inner-coated areas show an unstable behavior of the friction coefficient as documented in Fig. 5b. This observation indicates an oscillation between two sliding mechanisms presented during these tests; one with a lower and another one with a higher friction force.

The Fig. 6a shows a SEM image of worn and unworn regions on non-treated surface and one may distinguish the grooves on worn region and the wear direction. The edges of the wear tracks show the plastic deformation in the form of chips of the substrate.

Fig. 6b shows the approximate amount of oxygen (wt.%) on the worn surfaces after the wear test as detected by EDS. There is the clear trend for all three alloys that on remelted surface more oxides are formed during sliding in comparison with non-treated surface and the surface with injected WC particles contains more oxides after the wear test than the remelted one. The amount of oxygen detected on worn surfaces is a clear evidence of the presence of oxidation wear mechanism on all tested surfaces.

Fig. 7 shows an overview of the worn surface of non-treated 1A alloy characterized by confocal microscopy in order to measure the depth of worn groove (presented in Fig. 4a) and to evaluate its roughness in direction perpendicular to the sliding

direction. This roughness R_a was about 2.9 μm for non-treated and remelted surfaces and about 4.0 μm for surfaces with injected particles.

Advantaging of Z-contrast of BSE detector in the scanning electron microscope has been utilized to visualize a distribution of heavy and light elements on worn surfaces. Fig. 8 shows the BSE images of the worn surface of laser melt injected 3A alloy after the wear test as well as SE images of debris created on injected and non-treated surface, respectively.

Oxides (dark) are collected on WC particles (white) but also inside the grooves and holes on worn surface, as Fig. 8a shows. The debris formed on the injected surface also revealed a high level of oxidation and formed agglomerations shown in Fig. 8b. However, the substrate and remelting samples have shown wear debris characteristic for microcutting wear mechanism (Fig. 8c).

The more detailed observation of multigrain WC particles at worn surfaces revealed the intergranular fracture mechanism of their degradation. The clear evidence of a presence of this mechanism is shown in Fig. 9a, where a hole after intergranular fracture is present in the close vicinity of the WC grain, which was in a sliding contact during the final phase of the wear test. However, on some WC grains a clear evidence of plastic deformation in the form of shear bands has been detected (Fig. 9b).

The Fig. 10a and b compares the worn surface of the sample after injection with the worn surface of the non-treated sample. The oxides formed on the surface with WC particles clearly agglomerate in clusters with a size close to the size of injected particles.

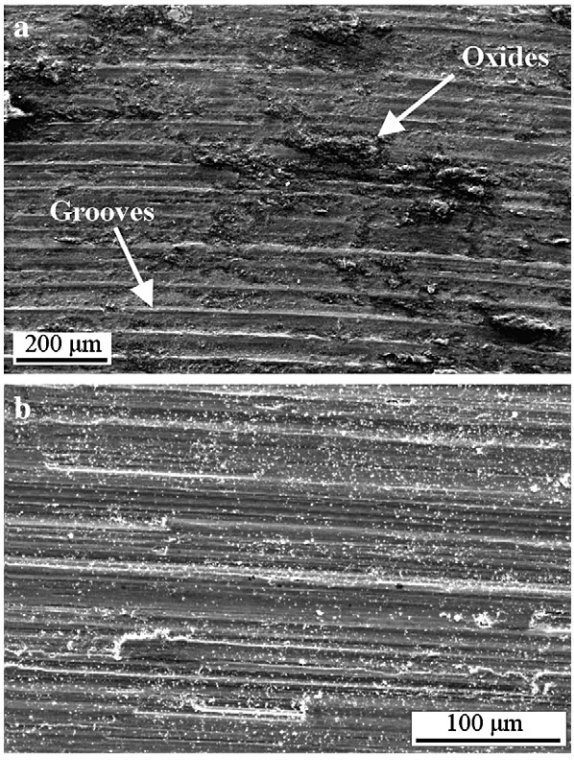

Fig. 10. The micrographs show details of worn surface — wear marks and debris. a) Significant oxides presented on wear track of DSS 3A after LMI. b) Less oxidized wear surface of DSS 6A in non-treated condition.

Table 2
The Relative Wear Resistance calculated from pin position measurement during wear test (RWR1) and from profile of worn groove after wear test (RWR2) for laser remelted and laser melt injected surfaces of all three alloys

Alloy	RWR1		RWR2	
	Remelted	WC_p injected	Remelted	WC_p injected
1A	1.6	2.9	1.9	6.7
3A	1.1	2.7	2.2	7.1
6A	2.7	5.9	2.3	7.3

4. Discussion

The reasons, why a quantification of improvement of wear resistance after injection ceramic particles into the metallic surface is not simple, were already addressed for MMC systems created at surfaces of aluminium and titanium alloys [3]. The measurement of pin position during the sliding wear test accompanies a large difference in wear of pin itself, when comparing wear behaviour of non-treated surface and MMC surface layer. Hard ceramic particles present in MMC may result in an intensive abrasive wear of pin, which is the reason why the relatively small differences in wear rates calculated from the pin position are observed. Nevertheless, there were large differences in depth of worn grooves. On the other hand, a comparison of wear rates calculated from the worn groove profile is distorted by the initial run-in behaviour, during which the wear rate may be much larger, than the wear rate during "stable" period. However, to quantify surface wear improvement after laser surface remelting and laser melt injection of WC particles into surface of three different duplex steel it is common to use the term "Relative Wear Resistance" defined as the wear rate of the non-treated surface divided by that of remelted or injected under same wear conditions [12]. Results are summarized in Table 2.

Both methods of the wear rate calculation lead to the conclusion that laser melt injection as well as the laser surface remelting enhances the dry sliding wear resistance of DCSS. Improvement in wear resistance after remelting is clearly connected with a small increase of hardness (see Fig. 5 in [9]) due to ferritization and finer microstructure formed by high cooling rates presented in laser processing [9]. The further hardness increase of the matrix (see Fig. 7 in [9]) due to dissolution of carbon and tungsten and the presence of WC particles well anchored in the matrix are responsible that the wear resistance of the MMC coating is even higher. A good bonding between matrix and WC particles is concluded from the fact that an intergranular fracture of individual grains from WC particle on worn surface is observed more often than holes, which may be attributed to the dropped out particle. Moreover, detailed microstructural observations [9] have shown that the reaction zone between injected WC particles and iron matrix exists. Such a reaction zone was confirmed many times to be sufficient for fair bonding [3,5,6] after LMI. Presented values of RWR for LMI surfaces of duplex steels are substantially lower

than values observed for injection of SiC and WC particles into Al and Ti alloys, tested at lubricated sliding wear. However, one may speculate that the injection of single grain WC particles of the same size as used in this experiment, will provide even more wear resistant WC/Duplex steel coating, because the main particle degradation process (intergranular fracture inside particles) observed in this work will be avoided.

When solid materials suffer from wear there is an accumulation of particles between rubbing surfaces. The so called "triboparticulates" originate from external contamination or accumulation of debris and can be encountered in the loose or compact format [13]. The effect of the triboparticulates on the wear mechanism is not completely clear and not very well understood. It can be confirmed that loose particles will act as abrasives and accelerate the wear damage while in the compacted form it reduces the wear considerably. In addition, the particulates can oxidize easily due to their small dimensions and relative large surface area, combined with their exposure to high temperatures. The oxidation can have a beneficial effect during the sliding of metals or alloys, when a compacted oxide layer is observed on the sliding tests performed and this effect is more pronounced [14].

EDS analysis of worn surfaces and debris collected at the end of wear tests confirmed a significant presence of oxygen. The sliding wear mechanisms accompanied by plastic deformation dominated on non-treated and remelted surfaces. During the wear at injected surfaces oxidation of metallic debris particle and mixed wear mechanism occur. A mixed wear mechanism is found at intermediate loading conditions with a production of both oxide and metallic debris. The heat of the deformation and the energy increase caused by the increase in the defect density and surface energy activates the oxidation. The oxide particles are agglomerated, which could protect the surface against subsequent wear loss. This interpretation is consistent with Jiang et al. [15], suggesting a model for the development of wear-protective oxide layers from the wear particles, ranging from room to high temperatures. A similar conclusion has been made in [16] about iron-rich oxide layers formed as a result of the machining of steel counterface by the particles that increase the wear resistance of ceramic particulate reinforced aluminium alloy composite by a factor of at least ten times.

The critical oxide layer thickness ε has been reported to be lower than 5 μm [17–19]. If one assumes the second case ($\varepsilon < d < 3\varepsilon$) of the Vardavoulias' approach [20], where d is mean size of one grain of multi-grains WC particles, only a small quantity of particles are removed together with oxides. However, when the oxide layer breaks up, most of the particles remain in the substrate and protude above the nominal surface. The pin will slide on these particles and the pin/second phase interaction takes place for some time. During this stage, which may be called the second stage of the wear mechanism (the first one is the formation and break of the oxide film) the matrix does not influence wear. The most important parameters are the mechanical resistance of the particles against the loading imposed by the pin and the strength of the matrix/particles bonding. The duration of this stage depends on whether the particles remain. The wear of the hard particles is low and the matrix is protected for a long period. This second stage wear may be accompanied by abrasion wear. It increases the friction coefficient to around 0.9 as shown the Fig. 5b. This behavior can be due to fracturing of the oxide film and leads to the forming of wear debris. The higher temperatures achieved on inner place may result in the production of more quantity of oxides, which after critical thickness come to break up. Then, another site elsewhere on the surface becomes operative. Areas of clean metallic surface come into rubbing contact and oxidize. The above described process starts again and the oxidative wear mechanism advances. One can see a ranging of friction coefficient between 0.4 and 0.9.

The traces of plasticity accumulated in WC particles can be explained due to the fact that injected particles support most of the load and the real contact area is therefore reduced which leads to a high contact stress. This higher contact stress leads to a higher local temperature being produced in the wear test for the LMI processed samples. This could relieve plastic deformation of WC even if the value of compressive yield stress of WC is almost thousand times higher than the nominal contact stress value calculated for this wear test. The increased temperature also accelerates the oxidation processes. The alloys 3A and 6A show higher wear resistance as well as oxide production on surface.

Using the BSE contrast in Fig. 11a the trapped oxidized debris close to WC particle may be observed. Two types of oxides present on worn surface may be distinguished. In literature three

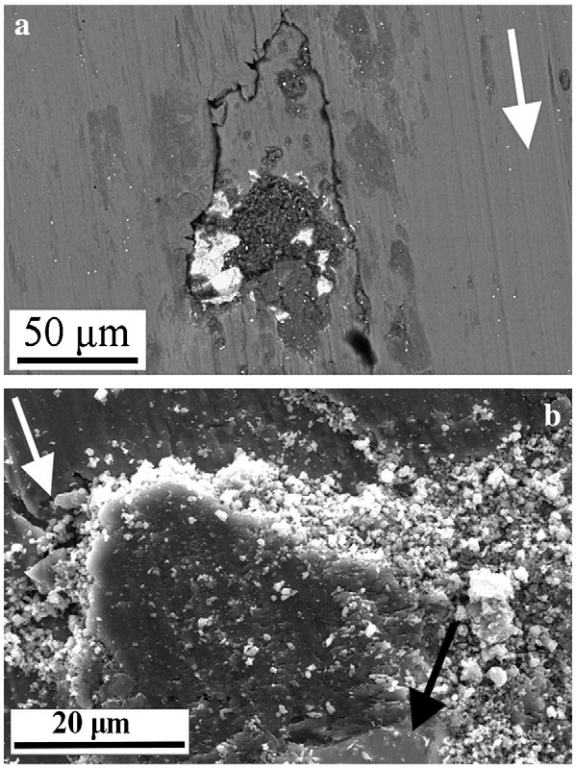

Fig. 11. a) BSE SEM micrograph exhibiting the presence of oxides on particle and close to the particle. Arrow indicates wear direction. b) SEM micrograph of worn surface of WC_p/DSSs tested at contact stress of 2.5 MPa. The white arrow indicates the wear direction, the black one shows the top of WC particle area, which was in a contact with pin. The WC_p works like barrier to movement of the debris.

different types of oxides with respect the produced contact temperatures are mentioned. Below 200 °C the major constituent is α-Fe_2O_3, for temperatures between 200 and 570 °C it is Fe_3O_4 and above 570 °C it is FeO [17]. In presented observations the predominant oxides in wear debris detected by EDS were probably α-Fe_2O_3 and Fe_3O_4. The relatively low sliding speed (0.1 m/s) did not allow the development of temperatures higher than 570 °C. The formation of α-Fe_2O_3 during dry sliding wear tests results in higher wear rates compared to Fe_3O_4, which produces a more protective surface film than the of α-Fe_2O_3. Fig. 11b shows the high concentration of oxidized debris close to the WC particle. The particle works as an obstacle to the movement of the triboparticulates in this case.

5. Conclusions

The study of dry sliding wear and friction behavior of the coatings created on three kinds of duplex stainless steels by laser surface remelting and laser melt injection of WC particles lead to the following conclusions:

- Laser surface remelting as well as laser melt injection of WC particles improves wear resistance of duplex steels;
- A substantial improvement in sliding wear resistance is observed for WCp/DSSs surface layers prepared by the LMI technique in comparison with non-treated and remelted surfaces;
- The amount of 10% of ceramic particles is sufficient to reinforce the matrix;
- The good bonding between injected WC particles and metal matrix induces intensive oxidation which forms a protective oxide layer;
- A localized plastic deformation near the contact surface of WC particles indicates high local contact stresses and temperatures during the wear test.

Acknowledgments

The work reported was carried at University of Groningen during a leave of absence from State University of Campinas by A.M. Do Nascimento. The authors acknowledge the financial support provided by The Scientific Research Foundation of the State of São Paulo, Brazil, FAEPEX-Unicamp, CNPq (The Brazilian Research Council), Capes and M2i – Materials Innovation Institute. Dr. Marcelo Martins from Sulzer Brazil S/A – Fundinox Division is acknowledged for providing with duplex steel experimental materials.

References

[1] R.N. Gunn, Duplex Stainless Steels – Microstructure, Properties and Applications, Abington Publishing, Cambridge, England, 1997, p. 204.
[2] J.H. Abboud, D.R.F. West, J. Mater. Sci. Lett. 10 (1991) 1149.
[3] V. Ocelík, D. Matthews, J.Th.M. De Hosson, Surf. Coat. Technol. 197 (2005) 303.
[4] J.A. Vreeling, V. Ocelík, Y. Pei, D. van Agterveld, J.Th.M. De Hosson, Acta Mater. 48 (2000) 4225.
[5] J.Th.M. De Hosson, V. Ocelík, Mater. Sci. Forum 123 (2003) 426.
[6] Y. Pei, V. Ocelík, J.Th.M. De Hosson, Acta Mater. 50 (2002) 2035.
[7] H. Hiraga, T. Inoue, S. Kamado, Y. Kojima, Mater. Trans. 42 (2001) 1322.
[8] M.H. Zhao, A.G. Liu, M.H. Guo, D.J. Liu, Z.J. Wang, C.B. Wang, Surf. Coat. Technol. 201 (2006) 1655.
[9] A.M. Do Nascimento, V. Ocelík, J.Th.M. De Hosson, Surf. Coat. Technol. 202 (2007) 2113.
[10] Y.T. Pei, D. Galvan, J.Th.M. De Hosson, Acta Mater. 53 (2005) 4505.
[11] M. Riabkina-Fishman, E. Rabkin, P. Levin, N. Frage, M.P. Dariel, A. Weisheit, R. Galun, B.L. Mordike, Mater. Sci. Eng. A302 (2001) 106.
[12] I.M. Hutchings, S. Wilson, A.T. Alpas, in: A. Kelly, C. Zweben (Eds.), Comprehensive Composite Materials, Pergamon, Amsterdam, 2000, p. 3.19.
[13] J.R. Jiang, F.H. Stott, M.M. Stack, Tribol. Int. 31 (1998) 245.
[14] Metals Handbook, 10th ed., v. 18, ASM, Ohio, 1990, p.280.
[15] J.R. Jiang, F.H. Stott, M.M. Stack, Wear 176 (1994) 185.
[16] J. Zhang, A.T. Alpas: Proc. Of the ASM Materials Congress, Materials Week '93, Pittsgurgh, Pensylvania, 1993, 65–77.
[17] T.F.J. Quinn, D.M. Rowson, J.L. Sullivan, Wear 65 (1980) 1.
[18] J.L. Sullivan, S.S. Athwal, Tribol. Int. 16 (1983) 123.
[19] Zum Gahr, K.H., Tribology Series 10, Elsevier Science Publishers B. V., 1987, p. 560.
[20] M. Vardavoulias, Wear 173 (1994) 105.